Disappearance of ferroelectric critical thickness in epitaxial ultrathin $BaZrO_3$ films

Yajun Zhang,[1] Gui-Ping Li,[1] Takahiro Shimada,[2] Jie Wang,[1,2,*] and Takayuki Kitamura[2]

[1]*Department of Engineering Mechanics, School of Aeronautics and Astronautics, Zhejiang University, Hangzhou 310027, China*

[2]*Department of Mechanical Engineering and Science, Kyoto University, Nishikyo-ku, Kyoto 615–8540, Japan*

(Received 5 August 2014; revised manuscript received 4 November 2014; published 20 November 2014)

The intrinsic critical ferroelectric thickness of epitaxial ultrathin capacitors of incipient ferroelectric $BaZrO_3$ (BZO) films with realistic $SrRuO_3$ (SRO) electrodes is investigated by first-principles calculations based on density functional theory. We reveal that polarization can stably exist even in one-unit-cell thick BZO films, i.e., absence of critical thickness, whereas the widely investigated proper ferroelectrics like $BaTiO_3$ and $SrTiO_3$ films have no polarization. The influences of realistic ferroelectric-electrode interface and misfit strain on the ionic and electronic structures of the BZO-SRO thin film system have been examined under the short-circuited boundary condition. It is found that the ionic polarization of conductive SRO electrodes can effectively strengthen the screening of bound charges at the interface, which greatly reduces the depolarization field in the BZO films. Furthermore, the epitaxial misfit strain remarkably enhances the polarization through the enhancement of hybridization of Zr and O electron orbitals, resulting in the disappearance of ferroelectric critical thickness. Our findings are beyond the critical thickness of proper ferroelectrics and are thus promising for future nanometer-scale ferroelectric device such as high-density ferroelectric memory.

DOI: 10.1103/PhysRevB.90.184107 PACS number(s): 77.80.bn

I. INTRODUCTION

Ferroelectric oxide materials have a wide range of technological applications for their various fascinating properties. In particular, ferroelectric ultrathin perovskite films have attracted much attention in recent years due to their potential applications in nonvolatile random access memories and high-density data storage devices [1,2]. Ferroelectric memories are promising for future ultrahigh-density information storage technology since the polarization switching occurs within 1 ns, which can notably enhance the data accessing performance of the device. Following a practical tendency towards high-density data storage technology, a continuing demand for further miniaturization of electronic components has been the major focus of researchers. To achieve this aim, one of the most important issues is how to maintain ferroelectricity when the component size reduces to the nanometer scale. Due to the intrinsic size effect and depolarization effect, ferroelectric thin films are usually restricted by a critical thickness below which the ferroelectric polarization inevitably disappears. The existence of ferroelectric critical thickness is due to the fact that the polarization of a ferroelectric thin film is often perpendicular to the surface in applications. Under such a situation, the incomplete screening of the bound charges at the ferroelectric-electrode interface creates a strong depolarization field, which could completely suppress and destabilize the ferroelectric polarization. Furthermore, the depolarization effect becomes stronger when the films become thinner. Thus, finding effective ways to overcome the size effect and improve ferroelectric stability of ultrathin films has sparked tremendous interest.

Previous studies have shown that for a given integration of electrode and perovskite material, its ferroelectric properties are affected by different electrical boundary conditions [3–6], specific atomic relaxations [7], interface properties [8,9], and epitaxial strains [10–12]. An experimental study indicates that ferroelectric polarization disappears in the thin film with a critical thickness of 10 nm [13]. The theoretical study on the critical thickness of ferroelectric thin films was carried out by Junquera and Ghosez [5] through first-principles density functional theory (DFT) calculations. The first-principles calculations show that an ultrathin $BaTiO_3$ (BTO) film loses its ferroelectricity at a critical thickness of 2.4 nm. Afterwards, a large number of first-principles calculations have been conducted to investigate the ferroelectric critical thickness [7–9,14–19]. Among those, Gerra *et al.* [7] found that ferroelectricity of BTO film between $SrRuO_3$ (SRO) electrodes is maintained in film three unit cells thick when considering the relaxation of ions in the electrodes. Polanco *et al.* predicted that Pt/$PbTiO_3$(PTO)/Pt film can stabilize at a ground state, and the polarization is enhanced in the oxide film with no ferroelectric critical size by breaking in-plane symmetry [19].

Although there are extensive theoretical and experimental investigations on the ferroelectric critical thickness of thin films, most of them focus on the proper ferroelectrics such as PTO and BTO. It is well known that ferroelectric polarization can also be driven by the misfit strain in incipient ferroelectric thin films epitaxially grown on the substrates with different lattice constants. In the previous paper [20,21], it has been demonstrated that incipient ferroelectrics, such as $SrTiO_3$ (STO) and $BaZrO_3$(BZO) thin films, exhibit a remarkable ferroelectric polarization when they are subjected to compressive or tensile misfit strain. Nevertheless, to the best of our knowledge, there is no theoretical and experimental report on the critical thickness of incipient ferroelectrics, which may behave in a different way from proper ferroelectrics. Therefore, it should be of great interest, both scientifically and industrially, to investigate whether ferroelectric property maintains in incipient ferroelectric ultrathin films.

In this paper, we explore the ferroelectric critical thickness in an incipient ferroelectric thin film using DFT calculations. The BZO thin film is taken as a representative because it exhibits a large polarization in the presence of a misfit strain

*Corresponding author: jw@zju.edu.cn

 ©2014 American Physical Society

[20]. A model of SRO/BZO/SRO thin film epitaxially grown on a $KTaO_3$ substrate is used to investigate the critical thickness for the existence of ferroelectricity. Unlike the traditional ferroelectrics such as BTO and PTO, the incipient ferroelectric BZO thin film was found to possess ferroelectric polarization even when its thickness decreases to one unit cell thick, i.e., absence of critical thickness, due to the ionic relaxation of realistic electrodes and misfit strain imposed by the substrate. The finding is beyond the critical thickness of proper ferroelectrics and is thus promising for future nanometer-scale ferroelectric devices such as a high-density ferroelectric memory element. To further understand the underlying mechanism for the existence of polarization in the one-unit-cell thick thin film, the effects of interface, ionic polarization, and epitaxial strain on the density of states (DOS), the electrostatic potential, and ferroelectric polarization are investigated and discussed in the following sections.

II. METHOD OF CALCULATIONS

The present first-principles calculations are performed within the framework of DFT using the projector-augmented wave (PAW) method, which is implemented in the Vienna *Ab initio* Simulation Package (VASP) [22]. The (001) − oriented BZO thin films sandwiched between two SRO electrodes are investigated in the present paper, which is similar to the configuration of BTO thin films in Ref. [5]. The periodically repeated electrode-ferroelectrics-electrode multilayers are described by the general formula of $[SrO\text{-}(RuO_2\text{-}SrO)_n/ZrO_2\text{-}(BaO\text{-}ZrO_2)_m]$, where n is fixed at six and m denotes the number of unit cells in the BZO layer ranging from one to eight. The calculations are carried out by employing a superlattice periodically repeated in three directions. The exchange-correlation potential is treated by local density approximation (LDA) [15,23]. The LDA better describes the lattice constants of perovskite oxides than the generalized gradient approximation Perdew-Burke-Ernzerhof (GGA-PBE) or Perdew-Wang (PW)91 [15], while both the LDA and GGA often underestimate the band gaps of insulators and semiconductors [24]. The hybrid Hartree-Fock density functionals can correctly reproduce the band gap and provide the accurate electronic states. However, the Hartree-Fock density functionals may fail to describe phase stability in oxide materials [25], which is not suitable for the present paper as it mainly focuses on the stability of the ferroelectric phase in perovskite oxide. We also conducted the calculations by using the GGA functionals. The calculation results show that the c/a ratio of the unit cell is overestimated; therefore, we choose LDA in our calculations. The approximation of LDA may underestimate the band gaps but will not influence the main results of the present paper. Careful test calculations show that a relatively high plane-wave cutoff energy of 600 eV gives well-converged results, thus enough to accurately describe the electronic properties. The Brillouin-zone integrations are carried out using a $7 \times 7 \times 1$ Monkhorst-Pack k-point mesh [26]. The structures are fully relaxed until the force on each atom is less than 0.01 eV/Å. The in-plane lattice constant of the films is set equal to the experimental value of $KTaO_3$ (3.983 Å) to simulate epitaxial growth on the $KTaO_3$ substrate [27], which can provide sufficient strain to sustain the polarization in bulk BZO. Relaxation of bulk BZO and SRO are performed along the [001] direction under the same constraint. The optimized structures are then used as the building blocks for the electrode-ferroelectrics-electrode multilayers.

III. RESULTS AND DISCUSSIONS

A. Polarization stability of SRO/BZO/SRO film

In this paper, we use $KTaO_3$ as the substrate that provides an epitaxial strain of 4.25%. This can increase the c/a ratio and induce the ferroelectric property of bulk BZO [20] with a polarization of about 36 $\mu C/cm^2$. To see whether ferroelectric polarization maintains in the BZO ultrathin film between SRO electrodes in the presence of the depolarizing field, the ground-state structures with different thicknesses and the given initial displacements are determined through structure relaxation. The atomic positions of both BZO films and electrodes along [001] direction are fully relaxed. The profiles of the cation-anion relative displacements for different thicknesses are shown in Figs. 1(a)–1(e). The initial spontaneous polarization points rightward in the figures. It is interesting to find that the relative displacements are still considerably large when $m = 1$, which means that the polarization can be stabilized with a thickness of about 4 Å. Besides, the rumpling parameter that defines the cation-oxygen separation along the polarization direction is small when the thickness is small. However, it becomes larger and more stable when the thickness increases. This is because the depolarization field becomes stronger as the film thickness decreases, which can suppress ferroelectric polarization. It should be noted that the rumpling or polarization is not uniform along the thickness. The rightward initial polarization leads to an enhancement of Zr-O relative displacements at the left interfaces and a reduction at the right interfaces, which are consistent with previous theoretical calculations [4,28]. Another interesting phenomenon is that the ferroelectric related relative displacements penetrate into the metal-oxygen electrodes. Furthermore, the penetrated displacements decay away from the interface to the interior electrodes. As shown in Fig. 1, the polarization induced by the ionic displacement penetrates into the electrodes, which results in bound charges in the electrodes. The incomplete compensation of bound charges creates a depolarizing field, which continues into the electrodes. Because the electrodes possess a finite screening length, the magnitude of the depolarizing field can be greatly reduced [7]. Although it has been reported that monolayer ferroelectric polymer thin films exist, the present one-unit-cell thick ferroelectric BZO thin film is much thinner than widely used ferroelectric perovskite thin films.

B. Effect of the ferroelectric-electrode interface on the polarization

Due to the strong interaction between the atoms at the interfaces, the ferroelectric polarization in the BZO film would be strongly affected by the interface properties. In previous theoretical calculations, it has been demonstrated that a strong interface bonding can impose restrictions on the soft-mode motion, which thereby affects the ferroelectric

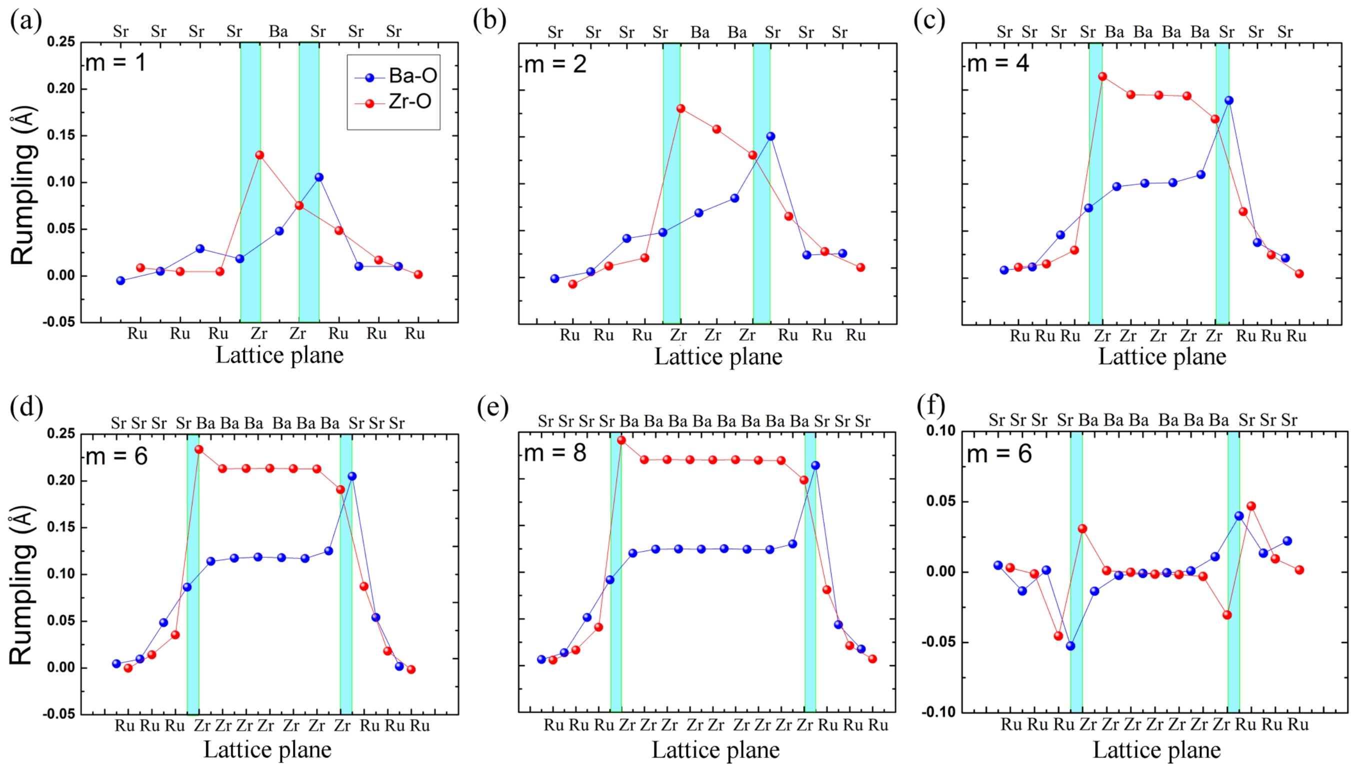

FIG. 1. (Color online) Atom layer rumpling (the relative displacement of cation-oxygen) profiles obtained from fully relaxed SRO/BZO/SRO thin films: (a)–(e) ferroelectric states with different thicknesses; (f) paraelectric state when $m = 6$.

critical thickness in the perovskite films [14]. To elucidate the effect of the interface on the BZO system, the paraelectric state is relaxed by imposing a mirror plane on the central ZrO_2 layer with an identical termination when $m = 6$. Figure 1(f) shows that the relaxations of ions and electrons at the interface induce interface dipoles even in the paraelectric state. Besides, the dipoles are perpendicular to the corresponding interfaces and point to opposite directions at two interfaces, which are consistent with previous calculations [14,29]. The antisymmetric interface dipoles are attributed to the antisymmetric rumpling of atoms at the interfaces of the electrode-ferroelectrics-electrode multilayer. Due to different work functions, charge transfer between the SRO and BZO layers exists, which may also produce antisymmetric electric dipoles at the interfaces [14].

The interface effect on the ferroelectric polarization of thin films with different thicknesses is also examined. It is found that the ferroelectric thin films have the same short-range characteristic at the interfaces as the paraelectric film. As shown in Figs. 1(a)–1(e), the magnitudes of polarization in the ferroelectric thin films are much larger than those of the interfacial dipoles induced by relative displacements in Fig. 1(f). Furthermore, a rightward initial polarization leads to an enhancement of Zr-O relative displacements at the left interfaces, while a reduction at the right interfaces. It should be noted that the relative displacements of Sr-O at the right interfaces are much larger. The enhancement of Sr-O rumpling at the right interfaces can be explained by the strong interaction between Zr and O at the interfaces. Figure 2 shows the local DOS of the atoms near the interface. The numbers "1–5" denote five Zr or O atoms at the right interface, which are shown by the schematic configuration in the left of Fig. 2. It is found that the electrons of O atom at the interfacial Sr-O layer redistribute relative to the internal O atom, and the hybridization between O p and Zr d states is enhanced.

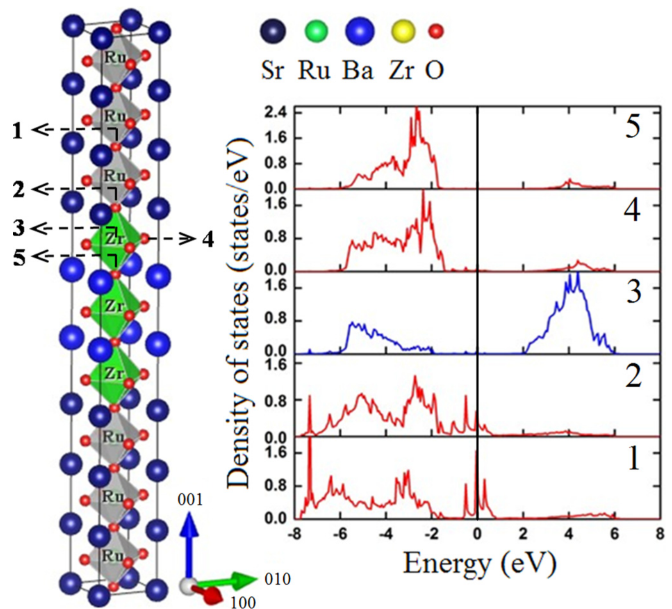

FIG. 2. (Color online) Schematic configuration and local DOS of a typical ferroelectric-electrode model in our calculation ($m = 2$). The atoms at the interface and adjacent to the interface are labeled by the numbers on the left, which correspond to those in DOS plots on the right. Fermi energy is set to zero energy.

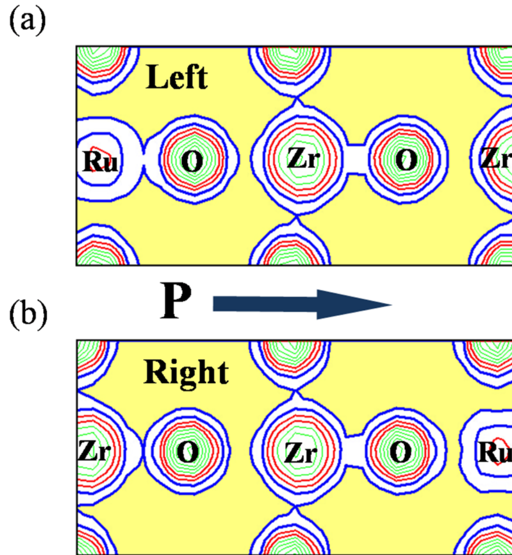

FIG. 3. (Color online) The calculated charge density for the interfacial atoms in the thin film with $m = 8$. The charge density is projected on the (100) plane to show the bond connection. The polarization direction is rightward.

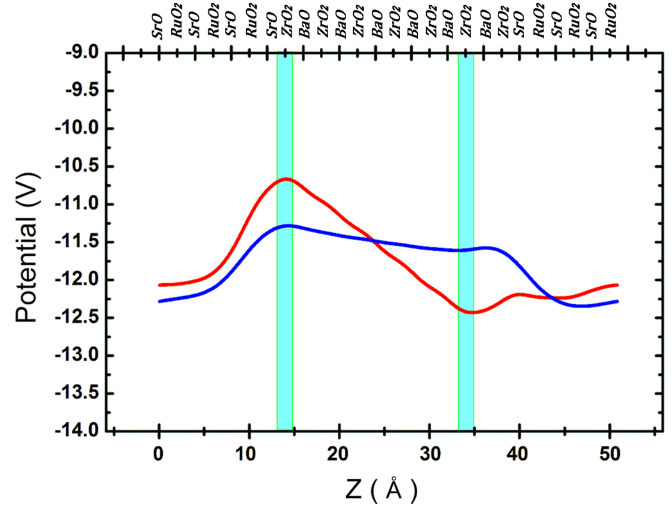

FIG. 4. (Color online) Macroscopic averages of the electrostatic potential of the thin film ($m = 6$) along the [001] direction. The blue curve is obtained when the ferroelectric-electrode structure is fully relaxed, while the red curve is obtained from the case with fixed electrodes.

Comparing the states of the 2 Op orbital with those of the 5 Op orbital, the hybridization between the Op orbital and the middle Zr d orbital at the Sr-O layer is stronger than that at the Ba-O layer. Correspondingly, the Zr-O (2) bond length along [001] direction at the interface is rather short, while another Zr-O(5) bond becomes significantly longer [30]. As shown in Fig. 3(b), in the presence of the rightward polarization, the Zr-O (Sr-O layer) bond at the right interface is much stronger than the adjacent Zr-O(Ba-Olayer) bond, whereas an opposite case occurs at the left interface, as shown in Fig. 3(a). Therefore, the distances between the interfacial atoms at the two interfaces are different due to the presence of initial polarization, which induces the difference in bond strength and causes the symmetry breaking.

C. Effect of ionic polarization on the depolarization field

To explain the disappearance of critical thickness in the present paper, the depolarization field is investigated in the thin film by plotting the macroscopic-averaged [31] electrostatic potential. In previous calculations, Junquera and Ghosez [5] revealed that BTO thin films between SRO electrodes lose ferroelectricity at a critical thickness of 24 Å based on the frozen-phonon method, in which the ionic relaxation of the electrodes is neglected. Then Gerra *et al.* [7] predicted that for the same SRO/BTO/SRO structure, the critical thickness can be down to 12 Å with the consideration of ionic relaxation. In our calculation, all the atomic positions are fully relaxed along [001] direction by using the same relaxation method as that in Ref. [7]. As is shown in Fig. 1, notable relative displacements can penetrate into the electrodes for a distance, which means that the polarization determined by the ionic displacements continues into the metal-oxide electrodes. It has been demonstrated that the ionic polarization of the electrodes plays an important role in stabilizing the ferroelectric phase in BTO with a twofold increase in the screening ability of electrodes [7]. However, this may not be a universal property for all the perovskite ferroelectrics such as PTO [28]. To determine whether ionic relaxation is effective in our system, the depolarization field of the fully relaxed structure is compared with that of structure freezing the ionic displacements of electrodes artificially. The depolarization field is calculated from the slope of the potential drop in the BZO slab. Figure 4 shows the electrostatic potential along the thickness, in which $m = 6$ is taken as an example. Among the two curves, the red curve is the potential of the fully relaxed structure, while the blue curve denotes the electrodes' fixed structure. It is found that the curves in the ferroelectric slab are not flat, which means that there still exists a depolarization field that can reduce the ferroelectric polarization at a finite size. Compared with the case of fixed electrodes, the depolarization field decreases significantly when the ionic relaxation in the electrodes is considered, which is shown by the two curves in Fig. 4. Surprisingly, it is found that the slope in the BZO film is more than five times smaller than that of the BTO film [7]. The reduction of the depolarizing field in the present model is attributed to the ionic polarization of electrodes, which is similar to that of the SRO/BTO/SRO superlattice in Ref. [7]. The inhomogeneous ionic polarization in electrodes generates bound charges in the electrodes, which can be compensated by the free electrons in the electrodes. Therefore, the ionic polarization of electrodes is responsible for the reduction of the depolarizing field [5]. The above result concludes that the ionic distortions within the electrodes can greatly decrease the depolarization field, which may be the primary cause of the disappeared critical thickness in the BZO thin film.

D. Strain dependence of polarization

In the above discussion, we have shown that the penetration of ionic displacements into the electrodes is responsible for

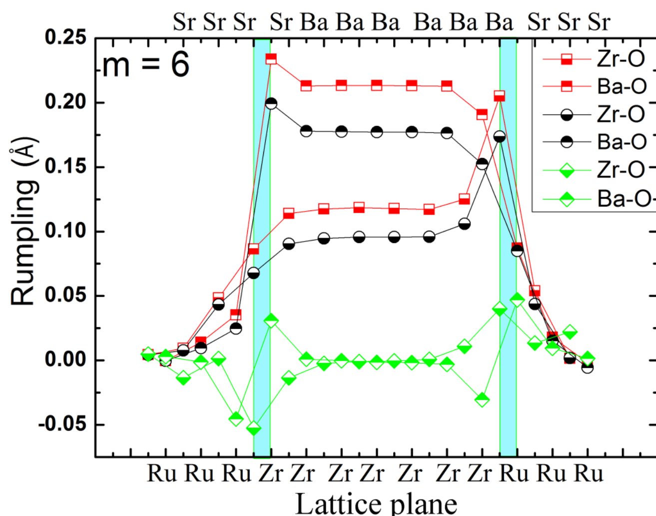

FIG. 5. (Color online) The rumplings of the thin film ($m = 6$) with different epitaxial strains. The red, black, and green symbols denote the results with $a = 3.983$ Å, $a = 4.013$ Å, and $a = 4.042$ Å, respectively.

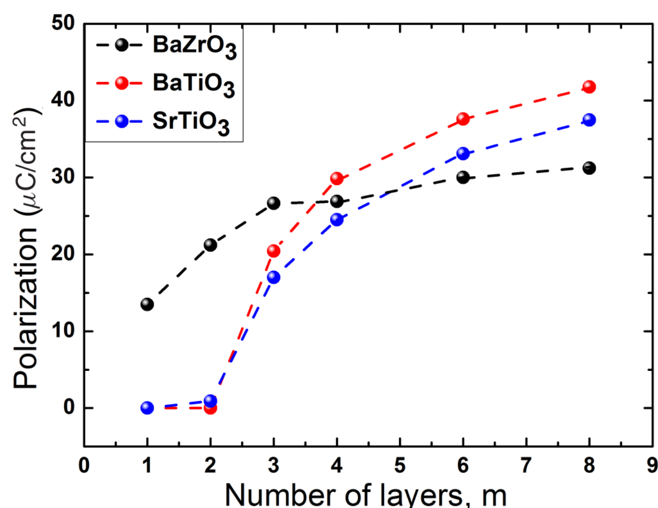

FIG. 6. (Color online) Dependence of polarization on the thickness of thin film. The polarizations in BTO and STO thin films disappear when the thickness is two-unit-cells thick, while the polarization in BZO is nonzero even when the thickness becomes one-unit-cell thick.

the great reduction of the depolarization field, which makes the spontaneous polarization a considerable value as the film thickness decreases. The epitaxial strain imposed by the substrate due to different lateral lattice constant is another important factor that can stabilize the polarization in the systems. Recently, a great interest has emerged in epitaxial ultrathin films of ferroelectric perovskite structure such as $Pb(Zr,Ti)O_3$, which have potential application in nanoelectronic high-density memory devices [32,33]. In general, the thinner the films, the higher the storage density will be. Thus, the epitaxially grown BZO film that can keep the ferroelectric at one-unit-cell thick may be an important candidate in the future high-density storage. It is well known that BZO crystal is paraelectric in the absence of strain. In a previous calculation [20], we have demonstrated that bulk BZO subjected to a critical compressive (or tensile) strain exhibits nontrivial spontaneous polarization, which is even higher than that of well-known ferroelectric BTO. To study the effect of epitaxial strain on the thin films, the lattice parameter of substrates gradually increases until a paraelectric state is obtained. Layer rumplings in the structures with varying lattice constants when $m = 6$ are plotted in Fig. 5, in which different colors and symbols denote different in-plane lattice constants. The red symbol denotes $a = 3.983$ Å, and the black and green symbols correspond to $a = 4.013$ Å and $a = 4.042$ Å, respectively. As shown in Fig. 5, the amplitude of the relative displacements of BZO films grown on different substrates decreases as the lattice parameter of substrate increases. The polarization decreases monotonically and finally disappears as the magnitude of epitaxial strain is reduced. In the present paper, the calculated cubic lattice constant 4.16 Å is taken as a reference state. When $a = 4.042$ Å in bulk BZO, the polarization is about 15 μC/cm^2 [20]. While in the thin film, the polarization is suppressed completely with this lattice constant. This result is induced by the depolarization field, which is perpendicular to the surface of the thin film and reduces the polarization stability. However, the polarization emerges and becomes stable when the magnitude of in-plane strain increases, which implies that the coupling between strain and polarization is very strong in the thin film. Therefore, the stable and large ferroelectric polarization can be achieved by choosing appropriate substrates. Based on the above results, the ionic polarization in the electrodes and epitaxial strain imposed by the substrate are essential in stabilizing the ferroelectric phase in BZO film.

E. Comparison with BTO and STO

In previous calculations, it has been demonstrated that the ferroelectric critical thickness of BTO thin film between SRO electrodes is three unit cells [7]. The present paper shows that the BZO film can still retain ferroelectricity down to as small as one-unit-cell thick. To further demonstrate the difference of BZO thin film from other perovskite thin films, the polarizations of BTO and STO films are also calculated under the same epitaxial strain and electrodes. Figure 6 gives the polarizations of BZO, STO, and BTO as a function of thickness. The polarization (per unit cell) is calculated from the Born effective charge as

$$P_i = \frac{e}{\Omega_c} \sum_j w_j Z_j^* \delta u_j, \quad (1)$$

in which P_i is the spontaneous polarization along the [001] direction. $\Omega_c, \delta u_j$ denote primitive cell volume and the displacements of atom relative to the centrosymmetric structure. Index j covers all atoms in the unit cell, and Z_j^* denotes the Born effective charge tensor calculated by density functional perturbation theory. Weights w_j are set to 1/8 for Ba, 1 for Zr, and 1/2 for O, which correspond to the number of unit cells that share the atom. As expected, the BTO film becomes paraelectric at $m = 2$ or less, while the polarization appears at the three-unit-cells thick or larger, which is consistent with a previous result [7]. This

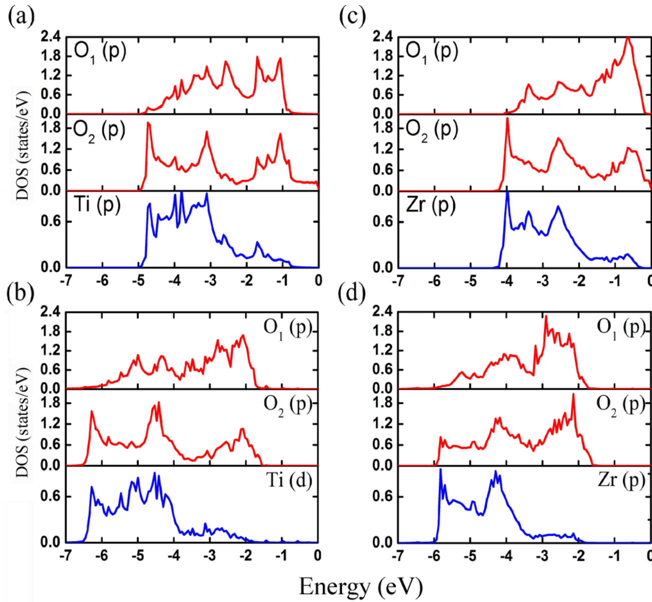

FIG. 7. (Color online) (a) Local densities of states for bulk BTO, (b) local DOS for BTO thin film ($m = 2$), (c) local DOS for bulk BZO, and (d) local DOS for BZO thin film ($m = 2$). The symbols O_1 and O_2 denote the DOS of O atoms parallel and perpendicular to the Ti(Zr)-O bond in the [001] direction, respectively. Fermi energy is taken for zero energy.

result shows that the ferroelectric property of BZO film is different from that of the proper ferroelectric BTO film. Why does two-unit-cells thick BTO film remain paraelectric while BZO film under the same conditions becomes ferroelectric? One effective way to understand this is to investigate the local DOS [34]. The calculated local DOS for BZO (BTO) bulk and thin film are shown in Fig. 7, respectively, in which the strains are the same, and $m = 2$. As shown in Figs. 7(a)–7(d), the energies of p electrons of the O atom and d electrons of the Ti (Zr) atom are mainly located in the same range. This means that Op and Ti (Zr) d almost have the same valence DOS, confirming the hybridization between O and Ti (Zr) atoms. However, we can clearly find that the overlap area of partial DOS of Ti d and Op in Fig. 7(a) is larger than that in Fig. 7(b). While in Figs. 7(c) and 7(d), the overlap area of partial DOS of Zr d and Op are nearly the same. So we can draw the conclusion that the hybridization between Ti and O atoms in the film is reduced compared to the hybridization in the bulk BTO. In other words, the interaction between the interfacial atoms is weaker in the film compared to bulk BTO. In contrast, the hybridization between O and Zr atoms in the BZO film is as strong as that in the bulk BZO. It is well known that a long-range Coulomb force and a short-range repulsion force exists in ferroelectrics. The strong hybridization between atoms can weaken the short-range repulsions and enhance the ferroelectric distortion [34]. Thus, the weaker interaction between Ti and O is the main reason that the BTO thin film loses ferroelectric property. As we mentioned in the Introduction, BZO is one kind of incipient ferroelectric. Can other incipient ferroelectrics under the same condition remain ferroelectric? To answer this question, we take the well-known perovskite STO as an example. The corresponding polarization is also shown in Fig. 6. Similar to BTO film, ferroelectricity emerges in STO film when the thickness is equal to or larger than three-unit-cells thick, which implies that the characteristic of losing critical thickness is not a universal property for incipient ferroelectrics. It should be noted that different terminations at interface would also affect the polarization of the thin film and even change the critical thickness. The effect of different terminations on the ferroelectric properties and critical thickness of BZO film is important and also interesting, which is worth investigating in the future. To the best of our knowledge, there are no experiments on the critical thickness of incipient ferroelectrics, especially on the BZO film, although many experiments have been conducted on the critical thickness of proper ferroelectrics [35–37]. Our findings may stimulate the interest of experimentalists to study this novel property of incipient ferroelectric BZO thin films.

IV. CONCLUSIONS

In conclusion, the ferroelectric critical thickness of BZO incipient ferroelectric thin film is investigated by first-principles calculations based on DFT. The first-principles calculations reveal that polarization can stably exist in the one-unit-cell thick BZO film sandwiched by SRO electrodes, the system of which is epitaxially grown on a $KTaO_3$ substrate, whereas the widely investigated BTO and STO films have no polarization under the same condition. The existence of ferroelectric distortion in one-unit-cell thick BZO films implies the disappearance of ferroelectric critical thickness. Detailed structural and electronic data show that the ionic polarization in the electrodes and epitaxial misfit strain imposed by the substrate play critical roles in stabilizing the ferroelectric polarization in the BZO films. The ionic polarization in the electrodes reduces the depolarization field, while the epitaxial misfit strain enhances the orbital hybridization of Zr and O electrons. The decrease of depolarization field and the enhancement of interaction between Zr and O atoms are essential for the disappearance of ferroelectric critical thickness in the BZO films. The one-unit-cell thick BZO ferroelectric ultrathin film holds promise for future nanometer-scale ferroelectric device such as the high-density ferroelectric memory element beyond the conventional proper ferroelectrics or dielectrics. Our findings will stimulate experimental investigation on this property of incipient ferroelectric BZO thin films.

ACKNOWLEDGMENTS

The authors acknowledge the financial support for J.W. from the National Natural Science Foundation of China (Grants No. 11321202 and No. 11472242), the Fundamental Research Funds for the Central Universities (Grant No. 2014FZA4027), and for T.S. and T.K. from the Grant-in-Aid for Specially Promoted Research (Grant No. 25000012) and the Grant-in-Aid for Scientific Research (B) (Grant No. 26289006) from the Japan Society for the Promotion of Science (JSPS).

[1] J. F. Scott, *Ferroelectric Memories*, Vol. 3 of Springer Series in Advanced Microelectronics (Springer-Verlag, Berlin, 2000).
[2] M. Dawber, K. M. Rabe, and J. F. Scott, Rev. Mod. Phys. **77**, 1083 (2005).
[3] P. Ghosez and K. M. Rabe, Appl. Phys. Lett. **76**, 2767 (2000).
[4] B. Meyer and D. Vanderbilt, Phys. Rev. B **63**, 205426 (2001).
[5] J. Junquera and P. Ghosez, Nature **422**, 506 (2003).
[6] I. Kornev, H. Fu, and L. Bellaiche, Phys. Rev. Lett. **93**, 196104 (2004).
[7] G. Gerra, A. K. Tagantsev, N. Setter, and K. Parlinski, Phys. Rev. Lett. **96**, 107603 (2006).
[8] D. D. Fong, A. M. Kolpak, J. A. Eastman, S. K. Streiffer, P. H. Fuoss, G. B. Stephenson, C. Thompson, D. M. Kim, K. J. Choi, C. B. Eom, I. Grinberg, and A. M. Rappe, Phys. Rev. Lett. **96**, 127601 (2006).
[9] M. Sepliarsky, M. G. Stachiotti, and R. L. Migoni, Phys. Rev. Lett. **96**, 137603 (2006).
[10] S. Tinte and M. G. Stachiotti, Phys. Rev. B **64**, 235403 (2001).
[11] O. Diéguez, S. Tinte, A. Antons, C. Bungaro, J. B. Neaton, K. M. Rabe, and D. Vanderbilt, Phys. Rev. B **69**, 212101 (2004).
[12] D. Cao, H.-B. Shu, Z.-W. Jiao, Y. Zhou, M.-G. Chen, M.-Q. Cai, and W.-Y. Hu, Phys. Chem. Chem. Phys. **15**, 14770 (2013).
[13] T. Maruyama, M. Saitoh, I. Sakai, T. Hidaka, Y. Yano, and T. Noguchi, Appl. Phys. Lett. **73**, 3524 (1998)
[14] C.-G. Duan, R. F. Sabirianov, W.-N. Mei, S. S. Jaswal, and E. Y. Tsymbal, Nano Lett. **6**, 483 (2006).
[15] Y. Umeno, B. Meyer, C. Elsässer, and P. Gumbsch, Phys. Rev. B **74**, 060101 (2006).
[16] A. K. Tagantsev, G. Gerra, and N. Setter, Phys. Rev. B **77**, 174111 (2008).
[17] M. Stengel, D. Vanderbilt, and N. A. Spaldin, Nat. Mater. **8**, 392 (2009).
[18] Y. Umeno, J. M. Albina, B. Meyer, and C. Elsässer, Phys. Rev. B **80**, 205122 (2009).
[19] M. A. M. Polanco, I. Grinberg, A. M. Kolpak, S. V. Levchenko, C. Pynn, and A. M. Rappe, Phys. Rev. B **85**, 214107 (2012).
[20] Y. Zhang, M. Liu, J. Wang, T. Shimada, and T. Kitamura, J. Appl. Phys. **115**, 224107 (2014).
[21] J. H. Haeni, P. Irvin, W. Chang, R. Uecker, P. Reiche, Y. L. Li, S. Choudhury, W. Tian, M. E. Hawley, B. Craigo, A. K. Tagantsev, X. Q. Pan, S. K. Streiffer, L. Q. Chen, S. W. Kirchoefer, J. Levy, and D. G. Schlom, Nature (London) **430**, 758 (2004).
[22] G. Kresse and J. Furthmüller, Comput. Mater. Sci. **6**, 15 (1996).
[23] D. M. Ceperley and B. J. Alder, Phys. Rev. Lett. **45**, 566 (1980).
[24] T. Shimada, T. Ueda, J. Wang, and T. Kitamura, Phys. Rev. B **87**, 174111 (2013).
[25] R. Grau-Crespo, H. Wang, and U. Schwingenschlögl, Phys. Rev. B **86**, 081101 (2012).
[26] H. J. Monkhorst and J. D. Pack, Phys. Rev. B **13**, 5188 (1976).
[27] H. Yokota, Y. Uesu, C. Malibert, and J.-M. Kiat, Phys. Rev. B **75**, 184113 (2007).
[28] N. Sai, A. M. Kolpak, and A. M. Rappe, Phys. Rev. B **72**, 020101 (2005).
[29] W. Chen, Y. Zheng, X. Luo, B. Wang, and C. Woo, J. Appl. Phys. **114**, 064105 (2013).
[30] M. Fechner, S. Ostanin, and I. Mertig, Phys. Rev. B **77**, 094112 (2008).
[31] A. Baldereschi, S. Baroni, and R. Resta, Phys. Rev. Lett. **61**, 734 (1988).
[32] J. F. Scott and C. A. P. de Araujo, Science **246**, 1400 (1989).
[33] R. Waser, *Nano Electronics and Information Technology: Advanced Electronic Materials and Novel Devices* (Wiley—VCH, Weinheim, 2003).
[34] R. E. Cohen, Nature **358**, 136 (1992).
[35] T. Tybell, C. H. Ahn, and J. M. Triscone, Appl. Phys. Lett. **75**, 856 (1999).
[36] D. A. Tenne, P. Turner, J. D. Schmidt, M. Biegalski, Y. L. Li, L. Q. Chen, A. Soukiassian, S. Trolier-McKinstry, D. G. Schlom, X. X. Xi, D. D. Fong, P. H. Fuoss, J. A. Eastman, G. B. Stephenson, C. Thompson, and S. K. Streiffer, Phys. Rev. Lett. **103**, 177601 (2009).
[37] D. D. Fong, G. B. Stephenson, S. K. Streiffer, J. A. Eastman, O. Auciello, P. H. Fuoss, and C. Thompson, Science **304**, 1650 (2004).